

# NPPB block of the intermediate-conductance $\text{Ca}^{2+}$ -activated $\text{K}^+$ channel

Bernard Fioretti<sup>a,\*</sup>, Emilia Castigli<sup>a</sup>, Isabella Calzuola<sup>a</sup>, Alexander A. Harper<sup>b</sup>,  
Fabio Franciolini<sup>a</sup>, Luigi Catacuzzeno<sup>a</sup>

<sup>a</sup>Dipartimento Biologia Cellulare e Molecolare, Università di Perugia Via Pascoli 1, I-06123 Perugia, Italy

<sup>b</sup>Division of Molecular Physiology, School of Life Sciences, University of Dundee, Dundee DD1 5EH, UK

Received 17 May 2004; accepted 18 June 2004

Available online 23 July 2004

## Abstract

We have shown that the  $\text{Cl}^-$  channel blocker 5-nitro-2-(3-phenylpropylamino) benzoic acid (NPPB) also blocks the intermediate-conductance  $\text{Ca}^{2+}$ -activated  $\text{K}^+$  ( $\text{IK}_{\text{Ca}}$ ) current in human leukemic HL-60 and glioblastoma GL-15 cell lines. The macroscopic  $\text{IK}_{\text{Ca}}$  current was activated by ionomycin plus 1-EBIO, and identified as intermediate conductance by being fully blocked by charybdotoxin, clotrimazole, nitrendipine (L-type  $\text{Ca}^{2+}$  channel blocker), and NS1619 ( $\text{BK}_{\text{Ca}}$  channel opener), but not by D-tubocurarine or TEA. The  $\text{IK}_{\text{Ca}}$  current was blocked by NPPB in a reversible dose-dependent manner, with an  $\text{IC}_{50}$  of 39  $\mu\text{M}$  in HL-60 and 125  $\mu\text{M}$  in GL-15 cells. The block of the  $\text{IK}_{\text{Ca}}$  current was also recorded at the single channel level in excised inside-out patches. As expected, NPPB also blocked the volume-activated  $\text{Cl}^-$  current expressed by GL-15 cells, with an  $\text{IC}_{50}$  of 44  $\mu\text{M}$ . The functional implications of  $\text{IK}_{\text{Ca}}$  current block by NPPB are discussed.

© 2004 Elsevier B.V. All rights reserved.

**Keywords:** Intermediate-conductance  $\text{Ca}^{2+}$ -activated  $\text{K}^+$  channel; NPPB;  $\text{Cl}^-$  current; HL-60 cell; GL-15 cell; Patch clamp recording

## 1. Introduction

NPPB (5-nitro-2-(3-phenylpropylamino) benzoic acid) is generally regarded as an inhibitor of  $\text{Cl}^-$  currents in a variety of cell types, with an  $\text{IC}_{50}$  ranging between 5 and 100  $\mu\text{M}$  (Jentsch et al., 2002; Schultz et al., 1999). Since its discovery NPPB has been widely used in functional studies to understand the role of  $\text{Cl}^-$  currents, particularly those activated by stretch or a rise in intracellular  $\text{Ca}^{2+}$  (Jentsch et al., 2002). NPPB, however, is not very selective for  $\text{Cl}^-$  currents. It has been demonstrated to block other ion channels such as nonselective cation channels, volume-sensitive basolateral  $\text{K}^+$  channels in epithelia,  $\text{Ca}^{2+}$  release-activated  $\text{Ca}^{2+}$  currents ( $\text{I}_{\text{crac}}$ ), L-type, voltage-gated  $\text{Ca}^{2+}$  currents, gap junction hemichannels, as well as activating the  $\text{BK}_{\text{Ca}}$  channels (Illek et al., 1992; Gribkoff et al., 1996; Doughty et al., 1998; Schultz et al., 1999; Li et al., 2000;

Eskandari et al., 2002). Here we show that NPPB blocks  $\text{IK}_{\text{Ca}}$  channels expressed in human leukemic HL-60 and glioblastoma GL-15 cell lines (Wieland et al., 1992; Ghanshani et al., 2000; Fioretti et al., 2004) with a similar potency of block to that reported for  $\text{Cl}^-$  channels in a variety of cells.

The  $\text{IK}_{\text{Ca}}$  channel is a member of the  $\text{Ca}^{2+}$ -activated  $\text{K}^+$  channel family, and displays a unitary conductance of 20–60 pS, in symmetrical  $\text{K}^+$ . It is distinguished from the functionally related  $\text{Ca}^{2+}$ -sensitive  $\text{SK}_{\text{Ca}}$  and  $\text{BK}_{\text{Ca}}$  channels of smaller (2–20 pS) and larger (100–250 pS) unitary conductance by its pharmacology, biophysics and physiology (Vergara et al., 1998; Castle, 1999). Thus, the  $\text{IK}_{\text{Ca}}$  channel is blocked by the scorpion venom toxin charybdotoxin, as well as by the antimycotic clotrimazole, and the antihypertensive L-type  $\text{Ca}^{2+}$  channel blocker nitrendipine (Jensen et al., 1998). In contrast, it is resistant to iberiotoxin, TEA, D-tubocurarine, and apamin, effective blockers of either  $\text{BK}_{\text{Ca}}$  or  $\text{SK}_{\text{Ca}}$  channels (Vergara et al., 1998; Castle, 1999). The  $\text{IK}_{\text{Ca}}$  channel is present in many tissues, playing important roles in the physiology of lymphocytes (prolifer-

\* Corresponding author. Tel.: +39 75 585 5750; fax: +39 75 585 5762.  
E-mail address: [fabiolab@unipg.it](mailto:fabiolab@unipg.it) (B. Fioretti).

ation and cytokine secretion), erythrocytes (volume control), and intestinal and airway epithelial cells (apical water and  $\text{Cl}^-$  secretion) (Jensen et al., 1998, 2001). Agents that block the  $\text{IK}_{\text{Ca}}$  channel activity have been proposed as potential therapeutic agents for sickle cell anaemia, cystic fibrosis, secretory diarrhoea, autoimmune diseases and restenosis (Jensen et al., 2001; Kohler et al., 2003). A better understanding of the pharmacological properties of this channel was therefore thought to be of interest.

## 2. Materials and methods

### 2.1. Cell culture

The GL-15 glioblastoma multiform cell line (Bocchini et al., 1991) was grown in minimum essential medium (MEM) supplemented with 10% heat-inactivated fetal bovine serum, 100 IU/ml penicillin G, 100  $\mu\text{g}/\text{ml}$  streptomycin, and 1 mM sodium pyruvate. The flasks were incubated at 37 °C in a 5%  $\text{CO}_2$ -humidified atmosphere. The medium was changed twice a week, and the cells were subcultured when confluent. For experimental purposes, cells were seeded in Petri dishes at  $100 \times 10^3$  cells/ml and electrophysiological recordings were performed between 1 and 3 days after seeding.

The human promyelocytic leukemic cell line HL-60 was grown in suspension in RPMI 1640 medium (GIBCO) containing 10% heat-inactivated fetal bovine serum, 2 mM L-glutamine, 100  $\mu\text{g}/\text{ml}$  streptomycin, and 100 IU/ml penicillin G at 37 °C in a 5%  $\text{CO}_2$ -humidified atmosphere. Cells were subcultured twice a week to maintain densities between 2 and  $10 \times 10^5$  cells/ml. HL-60 cells were made to adhere to Petri dishes for electrophysiological recording following established procedures (Wieland et al., 1992).

### 2.2. Electrophysiology

Whole-cell perforated and inside-out patch clamp configurations were used for electrophysiological recordings from HL-60 and GL-15 cells. Single-channel and whole cell currents were amplified with a List EPC-7 amplifier (List Medical, Darmstadt, Germany), and digitized with a 12 bit A/D converter (TL-1, DMA interface; Axon Instruments, Foster City, CA, USA). The pClamp software package (version 7.0; Axon Instruments) was used. For on-line data collection, macroscopic and single-channel currents were filtered at 5 and 0.5 kHz, and sampled at 20 and 200  $\mu\text{s}/\text{point}$ , respectively. Membrane capacitance measurements were made by using the Membrane Test routine of the pClamp software. Whole cell currents were routinely expressed as current densities ( $\text{pA}/\text{pF}$ ) calculated with respect to the measured cell membrane capacitance. In assessing the dose–response curves shown in Figs. 1B, 2B, and 3C, the voltage errors due to uncompensated series

resistance ( $R_s$ ) were taken into account. Specifically, the effective voltage sensed by the membrane ( $V_{\text{real}}$ ) was calculated by subtracting from the applied voltage ( $V_{\text{com}}$ ) the amount of voltage drop across  $R_s$  ( $IR_s$ , where  $I$  is the current being measured):  $V_{\text{real}} = V_{\text{com}} - IR_s$ .

### 2.3. Solutions and drugs

Macroscopic currents were recorded using the perforated-patch method. The bathing Physiological Salt Solution (PSS) consisted of (in mM): NaCl 106.5, KCl 5,  $\text{CaCl}_2$  2,  $\text{MgCl}_2$  2, MOPS 5, glucose 20, Na-Gluconate 30 at pH 7.25, and the pipette solution was:  $\text{K}_2\text{SO}_4$  57.5, KCl 55,  $\text{MgCl}_2$  5, MOPS 10 at pH 7.2. Electrical access to the cytoplasm was achieved by adding amphotericin B (200  $\mu\text{M}$ ) to the pipette solution. Access resistances in the range 10–20 M $\Omega$  were achieved within 10 min following seal formation. In studies of GL-15 cells, octanol (1 mM) was added to the external bathing solution to block gap-junctions (Eskandari et al., 2002). Hypotonic solutions were prepared by mixing control bath solution with bath solution in which NaCl had been omitted. In inside-out single-channel recordings the bathing solution was: NaCl 135, KCl 5, MOPS 5,  $\text{MgCl}_2$  1,  $\text{CaCl}_2$  0.65, EGTA 1, glucose 10, octanol 1, at pH 7.2 (the estimated free  $\text{Ca}^{2+}$  concentration was 300 nM), and the pipette solution was: KCl 145,  $\text{MgCl}_2$  1, MOPS 5, EGTA-K 1, at pH 7.25. All chemicals used were of analytical grade. Dimethyl sulfoxide (DMSO), TEA, D-tubocurarine, clotrimazole, and NS1619 (1,3-Dihydro-1-[2-hydroxy-5-(trifluoromethyl)phenyl]-5-(trifluoromethyl)-2H-benzimidazol-2-one) were purchased from Sigma (St. Louis, MO, USA). Charybdotoxin was from Alomone Labs (Jerusalem, Israel). Ionomycin, 1-ethyl-2-benzimidazolinone (1-EBIO), nitrendipine, NPPB were purchased from Tocris Cookson (Bristol, UK). Clotrimazole, NS1619 and nitrendipine were prepared in DMSO (20 mM). NPPB, 1-EBIO, ionomycin and amphotericin B were similarly dissolved in DMSO to concentrations of 100, 100, 1 and 50 mM, respectively. Pharmacological agents were dissolved daily in the appropriate solution at the concentrations stated, and were bath applied by gravity-fed superfusion at a flow rate of 2 ml/min, with complete solution exchange within the recording chamber in around 1 min. The maximal DMSO concentration in the recording solution was about 1%. Experiments were carried out at room temperature (18–22 °C). Data are presented as mean  $\pm$  SE.

## 3. Results

The action of NPPB on the  $\text{IK}_{\text{Ca}}$  currents was investigated in HL-60 and GL-15 cell lines in whole-cell perforated, and inside-out patch clamp configurations. In perforated configuration the HL-60 and GL-15 cells were bathed in PSS. Stable  $\text{IK}_{\text{Ca}}$  current activation was achieved by applying the  $\text{Ca}^{2+}$ -ionophore ionomycin (0.5  $\mu\text{M}$ ) plus

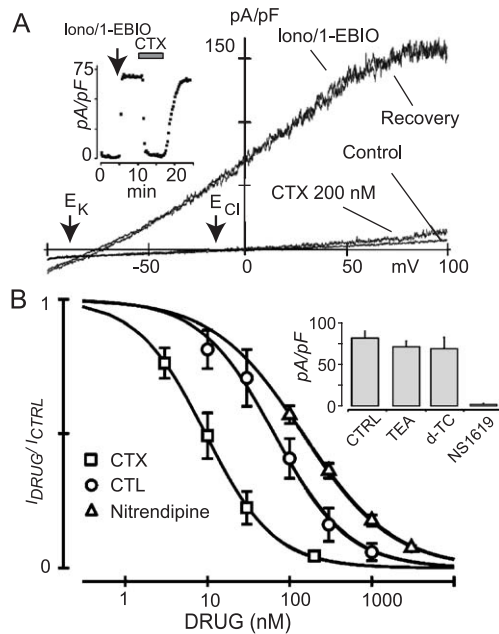


Fig. 1.  $I_{KCa}$  currents in HL-60 cells. (A) Current–voltage relationships recorded from a HL-60 cell in the perforated-patch configuration upon applying voltage ramps (from  $-100$  to  $+100$  mV, 800 ms duration), from a holding potential of 0 mV, first in control conditions, and then following application of ionomycin ( $0.5$   $\mu$ M) plus 1-EBIO ( $1$  mM), charybdotoxin (CTX,  $200$  nM), and recovery, in the continuous presence of ionomycin/1-EBIO. Inset: Time course of current activation by ionomycin/1-EBIO, block by charybdotoxin ( $200$  nM), and recovery, at 0 mV. (B) Mean fractional ionomycin/1-EBIO-induced current vs. drug concentration, [DRUG], at 0 mV. The solid lines represent the best fit of the experimental data with the Hill relationship:  $I_{DRUG}/I_{CTRL} = 1/[1 + ([DRUG]/IC_{50})^h]$ , where  $I_{DRUG}/I_{CTRL}$  is the fractional current induced by ionomycin/1-EBIO at varying drug concentrations with respect to control,  $IC_{50}$  is the half inhibitory concentration, and  $h$  is the Hill coefficient. Squares: charybdotoxin (CTX,  $IC_{50}=9.5$  nM,  $h=1.0$ ;  $n=4$ ); circles: clotrimazole (CTL,  $IC_{50}=64.7$  nM,  $h=0.97$ ;  $n=4$ ); triangles: nitrendipine ( $IC_{50}=144$  nM,  $h=0.8$ ;  $n=5$ ). Inset: Mean current density recorded at 0 mV under control conditions, and in presence of either TEA ( $2$  mM,  $n=3$ ), D-tubocurarine (D-TTC,  $100$   $\mu$ M,  $n=3$ ) or NS1619 ( $100$   $\mu$ M,  $n=3$ ).

the  $SK_{Ca}/I_{KCa}$  channel opener 1-EBIO ( $1$  mM) (ionomycin/1-EBIO). In both cell lines application of ionomycin alone resulted in a transient  $I_{KCa}$  current activation which was not suitable for our pharmacological tests. A typical experiment on HL-60 cell line demonstrating that application of ionomycin/1-EBIO resulted in the activation of a current ( $72$  pA/pF at 0 mV) is shown in Fig. 1A. The reversal potential of this current,  $E_{rev}$ , as assessed using voltage ramps from  $-100$  to  $+100$  mV from a holding potential of 0 mV, was  $-83$  mV, close to the calculated  $E_K$  of  $-90$  mV, for these recording conditions. The mean amplitude of the ionomycin/1-EBIO-activated current (at 0 mV), and mean  $E_{rev}$  were: HL-60,  $83.2 \pm 7.9$  pA/pF, and  $-77.0 \pm 0.9$  mV ( $n=17$ ); GL-15,  $6.9 \pm 1.3$  pA/pF, and  $-81.7 \pm 1.6$  mV ( $n=6$ ). The ionomycin/1-EBIO-activated current was fully, and reversibly, blocked by bath application of the  $I_{KCa}$  channel blocker charybdotoxin ( $200$  nM; Fig. 1A). The half-maximal blocking concentration,  $IC_{50}$ , for charybdotoxin was  $9.4$  nM (Fig. 1B). The ionomycin/1-EBIO-activated

current was also blocked by the other recognised  $I_{KCa}$  channel blocker clotrimazole and by the L-type  $Ca^{2+}$  channel blocker nitrendipine with  $IC_{50}$  of  $64.7$  and  $144$  nM, respectively, in good agreement with values reported for cloned and native  $I_{KCa}$  channels. Interestingly, the  $BK_{Ca}$  channel opener NS1619 ( $100$   $\mu$ M) also suppressed the whole-cell outward current. The current however, was insensitive to TEA (up to  $2$  mM) and D-tubocurarine (up to  $100$   $\mu$ M), effective inhibitors of the  $BK_{Ca}$  and the  $SK_{Ca}$  channels, respectively (Fig. 1B, inset). The biophysical and pharmacological profile of the ionomycin/1-EBIO-activated current in HL-60 cell line identifies it as an essentially pure  $I_{KCa}$  current, in line with previous work (Wieland et al., 1992). The ionomycin/1-EBIO-activated  $I_{KCa}$  currents of GL-15 cells were similarly blocked by these agents (data not shown; also cf. Fioretti et al., 2004).

NPPB inhibited the  $I_{KCa}$  current of HL-60 cells in a concentration dependent manner (Fig. 2). A representative experiment in which bath addition of  $200$   $\mu$ M NPPB almost completely blocked the  $I_{KCa}$  current, activated by prior

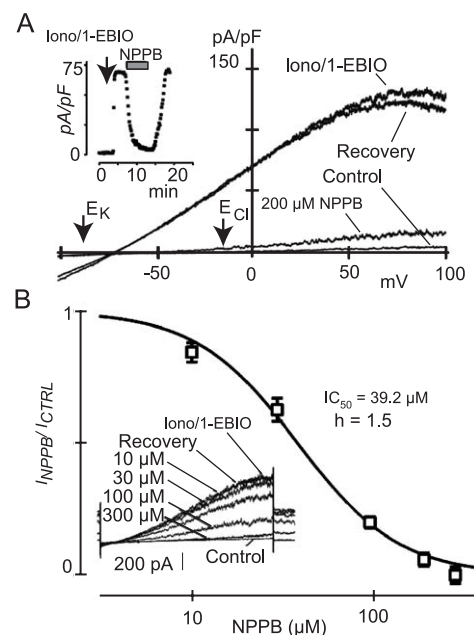


Fig. 2. NPPB blocks the  $I_{KCa}$  current of HL-60 cells. (A) Current–voltage relationships obtained from an HL-60 cell by applying voltage ramps (from  $-100$  to  $+100$  mV, 800 ms duration) in the perforated-patch configuration, from a holding potential of 0 mV, in control conditions, and after application of ionomycin ( $0.5$   $\mu$ M)/1-EBIO ( $1$  mM), and then NPPB ( $200$   $\mu$ M) in the continued presence of ionomycin/1-EBIO. Inset: Time course of current activation by ionomycin/1-EBIO, block of NBBP ( $200$   $\mu$ M), and recovery at 0 mV. (B) Plot of the mean fractional ionomycin/1-EBIO-induced current vs. [NPPB] ( $n=3-4$ ). The solid line represents the best fit of the experimental data with the Hill relationship:  $I_{NPPB}/I_{CTRL} = 1/[1 + ([NPPB]/IC_{50})^h]$ , where  $I_{NPPB}/I_{CTRL}$  is the fractional current induced by ionomycin/1-EBIO at varying NPPB concentrations with respect to control,  $IC_{50}$  is the half inhibitory concentration, and  $h$  is the Hill coefficient. The best-fit parameters were:  $IC_{50}=39.2$   $\mu$ M and  $h=1.5$ . Inset: voltage ramps (from  $-100$  to  $+100$  mV, 800 ms duration) from a holding potential of 0 mV showing the effect of varying NPPB concentration on the  $I_{KCa}$  current.

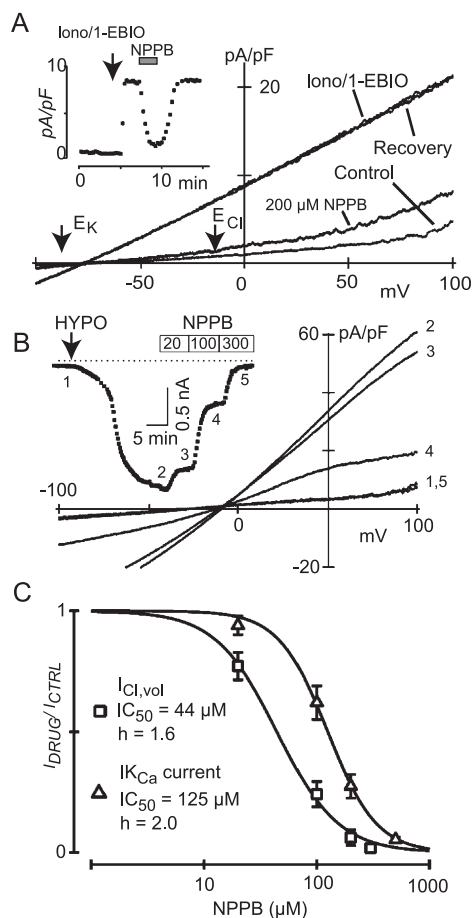


Fig. 3. NPPB blocks the  $I_{\text{KCa}}$  and  $I_{\text{Cl,vol}}$  current of GL-15 cells. (A) Current-voltage relationships obtained from a GL-15 cell by applying voltage ramps (from  $-100$  to  $+100$  mV, 800 ms duration) in perforated-patch configuration, from a holding potential of 0 mV, in control conditions, and after application of ionomycin ( $0.5$  μM)/1-EBIO ( $1$  mM), and NPPB ( $200$  μM) in succession, in the continuous presence of ionomycin/1-EBIO. Recovery from block is also shown. Inset: Time course of current activation by ionomycin/1-EBIO, block by NPPB  $200$  μM, and recovery from block, at 0 mV. (B) Current-voltage relationships obtained by applying voltage ramps (from  $-100$  to  $+100$  mV, 800 ms duration) in perforated-patch configuration, from a holding potential of 0 mV, in control conditions, in hypotonic solution (30% reduced extracellular osmolarity) to activate  $I_{\text{Cl,vol}}$ , and at varying NPPB concentrations. Inset: Time course of current activation by hypotonic solution and block by NPPB, at  $-80$  mV. The arrow indicates the time of application of the hypotonic solution, and the horizontal bars indicate the NPPB concentrations applied. The numbers indicate the times at which the corresponding current ramps of panel B were taken. (C) Concentration-response plot of NPPB inhibition of  $I_{\text{Cl,vol}}$  and  $I_{\text{KCa}}$  currents in GL-15 cells. Each data point represents the normalized mean current inhibition obtained at the indicated NPPB concentration. Data for  $I_{\text{KCa}}$  currents were obtained using a protocol similar to that shown in panel A, and data for  $I_{\text{Cl,vol}}$  currents were obtained with the protocol shown in the Inset. The solid line represents the best fit of the experimental data with the Hill relationship:  $I_{\text{NPPB}}/I_{\text{CTRL}} = 1/[1 + ([\text{NPPB}]/\text{IC}_{50})^h]$ , where  $I_{\text{NPPB}}/I_{\text{CTRL}}$  is the residual current at varying NPPB concentrations with respect to control,  $\text{IC}_{50}$  is the half inhibitory concentration, and  $h$  is the Hill coefficient. Squares:  $I_{\text{Cl,vol}}$  currents ( $\text{IC}_{50} = 44$  μM,  $h = 1.6$ ;  $n = 3-4$ ); triangles:  $I_{\text{KCa}}$  currents ( $\text{IC}_{50} = 125$  μM,  $h = 2.0$ ;  $n = 3-4$ ).

application of ionomycin/1-EBIO is shown in Fig. 2A and inset. NPPB block could be fully reversed on washout. Fig. 2B shows the concentration dependence of NPPB block of the  $I_{\text{KCa}}$  current. Data points (at 0 mV), representing the mean normalized residual  $I_{\text{KCa}}$  current at varying NPPB concentrations, were obtained from voltage ramps (shown in inset) and were fitted with a Hill relationship, giving an  $\text{IC}_{50}$  of  $39.2$  μM and a Hill coefficient of 1.5 (Fig. 2B).

NPPB blocked  $I_{\text{KCa}}$  and the volume-activated  $\text{Cl}^-$  current ( $I_{\text{Cl,vol}}$ ) in GL-15 cells with similar potency.  $I_{\text{KCa}}$  current elicited in GL-15 cells by application of ionomycin/1-EBIO was blocked by NPPB, see Fig. 3A. Concentration-response data assessed using the same experimental protocol used for HL-60 cells are shown in Fig. 3C, together with the best fit Hill relationship, giving an  $\text{IC}_{50}$  of  $125$  μM and a Hill coefficient of 2.0. In these cells we also recorded the  $I_{\text{Cl,vol}}$ , typical of many glioma cell lines (Ransom et al., 2001), and compared the efficacy of NPPB block of this current with that found for  $I_{\text{KCa}}$  current (Fig. 3B and C).  $I_{\text{Cl,vol}}$  could be activated by a 30% reduction in extracellular osmolarity (hypo) as shown in Fig. 3B. The reversal potential of the volume-activated current was  $-5$  mV, a value close to  $E_{\text{Cl}}$  for these recording conditions ( $-6$  mV; hypotonic conditions). As already shown in other glioma cell lines (Ransom et al., 2001), NPPB inhibited the  $I_{\text{Cl,vol}}$  in a concentration-dependent fashion (Fig. 3B and C). Fitting

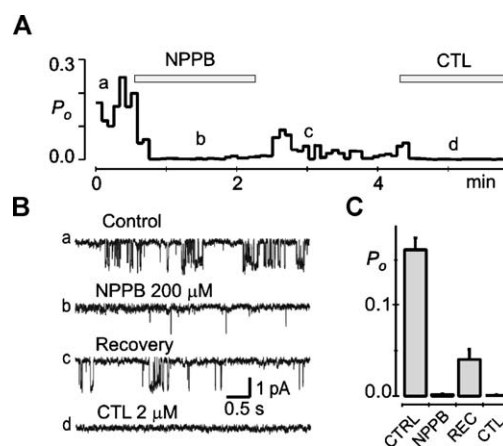


Fig. 4. NPPB blocks single  $I_{\text{KCa}}$  channels in GL-15 cell. (A) Running  $P_o$  (open probability) assessed over consecutive 5 s intervals of a continuous recording from an isolated patch in the inside-out configuration showing  $I_{\text{KCa}}$  channel inhibition by intracellular application of  $200$  μM NPPB, partial recovery after 2 min, and subsequent block by  $2$  μM clotrimazole. The pipette contained  $145$  mM KCl solution, and the intracellular face was bathed with a solution containing  $\text{Na}^+$  as the main salt, and a  $\text{Ca}^{2+}$  concentration of  $300$  nM (cf. Materials and methods). The applied membrane potential was  $-60$  mV. (B) Single-channel recordings taken from the same experiment of panel A, in control conditions (a), during NPPB ( $200$  μM) application (b), after partial recovery from the block (c), and in clotrimazole (CTL,  $2$  μM) (d). (C) Bar histogram showing the mean  $I_{\text{KCa}}$  channel  $P_o$  in the inside-out configuration assessed in control conditions ( $n = 4$ ), in NPPB ( $200$  μM;  $n = 4$ ), after recovery ( $n = 4$ ), and in clotrimazole ( $2$  μM;  $n = 2$ ).



the blocking efficacy at varying NPPB concentrations with a Hill relationship yielded an  $IC_{50}$  of 44.4  $\mu$ M and a Hill coefficient of 1.6 (Fig. 3C).

Finally, we tested the effect of NPPB on excised inside-out patches from GL-15 cells ( $n=4$ ), and found full block of unitary  $IK_{Ca}$  currents by the agent at comparable concentrations found to be effective in blocking macroscopic  $IK_{Ca}$  currents recorded in the perforated whole-cell mode. Recordings from inside out patches of GL-15 cells normally presented single-channel activity with unitary conductance, voltage- and  $Ca^{2+}$ -dependence typical of that for  $IK_{Ca}$  channels (Fioretti et al., 2004). Fig. 4 shows an inside-out recording where 200  $\mu$ M NPPB blocked a channel displaying such characteristics. In all cases examined the blocking action of NPPB could be partially reversed on drug washout. In two patches we were fortunate that the recording lasted long enough to further confirm the channel's identity by testing its sensitivity to clotrimazole (2  $\mu$ M; cf. Fig. 4A). We were never able to obtain a substantial recovery from the inhibitory effect of clotrimazole. Fig. 4B illustrates representative unitary current records obtained for these various manoeuvres. The bar histogram shows the average  $P_o$  (assessed at  $-60$  mV) under these experimental conditions (indicated).

#### 4. Discussion

In this paper we provide evidence that the  $Cl^-$  channel blocker NPPB also effectively blocks the macroscopic  $IK_{Ca}$  current activated in HL-60 and GL-15 cell lines by bath-application of ionomycin/1-EBIO, and the  $IK_{Ca}$  unitary activity on excised inside-out patches (GL-15). The ionomycin/1-EBIO-activated current displays a pharmacological profile consistent with that reported for both native and cloned  $IK_{Ca}$  currents in several tissues (Jensen et al., 1998; Warth et al., 1999; Castle, 1999). The block of the  $IK_{Ca}$  current by NPPB had a  $IC_{50}$  of 39.2 and 125  $\mu$ M in HL-60 and GL-15 cells, respectively. Similar blocking potency is displayed by NPPB for several types of  $Cl^-$  channels, such as the cystic fibrosis transmembrane conductance regulator (CFTR),  $I_{Cl,vol}$ , and  $Ca^{2+}$ -activated  $Cl^-$  current (all blocked by NPPB in the micromolar range: 5  $\mu$ M  $< IC_{50} < 100$   $\mu$ M; reviewed by Jentsch et al., 2002). Our data show that NPPB blocks  $IK_{Ca}$  and  $I_{Cl,vol}$  currents in GL-15 cells with a comparable potency. This is especially relevant to the many experimental models in which  $IK_{Ca}$  and NPPB-sensitive  $Cl^-$  channels are coexpressed, and contribute to important regulatory mechanisms such as volume regulation, and related processes such as cell proliferation and migration (Schwab, 2001; Okada et al., 2001). Our observations would thus reinforce the notion that caution must be exercised in the functional interpretation of data using this agent (cf. Introduction). The Hill number of the  $IK_{Ca}$  current block by NPPB measured 1.5 in HL-60 and 2.0 in GL-15 cells. These values

are similar to the Hill number we obtained for NPPB block of  $I_{Cl,vol}$  currents in GL-15 cells (about 1.6), but significantly higher than those obtained for the classical  $IK_{Ca}$  channel inhibitors (such as charybdotoxin, clotrimazole and nitrendipine, all showing a Hill slope close to 1). These results suggest that the block of both  $IK_{Ca}$  and  $I_{Cl,vol}$  currents by NPPB may originate from a common mechanism, distinct from that of the classical  $IK_{Ca}$  channel blockers, showing Hill numbers close to 1.

Indications for the block of  $IK_{Ca}$  channels by NPPB can be found in the literature. A volume-activated basolateral  $K^+$  channel in HT-29/B6 monolayers has been reported to be inhibited by NPPB with an  $IC_{50}$  of 114  $\mu$ M (Illek et al., 1992). Volume-activated  $IK_{Ca}$  currents are present in the basolateral membrane of many epithelia (Warth et al., 1999). In the basolateral membrane of human colonic crypt cells, a low-conductance  $Ca^{2+}$ -activated  $K^+$  channel, possibly  $IK_{Ca}$ , was found to be blocked by the NPPB analog diphenylamine-2-carboxylate (DPC; Richards and Dawson, 1993). Together, these observations may suggest that NPPB can block a volume-activated  $IK_{Ca}$  current in the basolateral membrane of certain epithelia. A recent report shows that in IGR1 melanoma cells NPPB blocks a  $K_{Ca}$  current most likely associated with  $IK_{Ca}$  channels (Gavrilova-Ruch et al., 2002).

In several instances NPPB has been used as a blocker of  $I_{Cl}$  currents, to study the  $IK_{Ca}$  channel in isolation. For this purpose, NPPB has been used at concentrations (50  $\mu$ M; Wang et al., 2003) comparable to the  $IC_{50}$  of NPPB block of  $IK_{Ca}$  we found in this study. In contrast, in another study a much higher concentration than the  $IC_{50}$  of NPPB block we report here for  $IK_{Ca}$  was used (500  $\mu$ M; Khanna et al., 2001), without affecting  $K_V$  or  $SK_{Ca}$ -like  $K^+$  channel activity. We do not have an explanation for these apparently conflicting results.

The  $IK_{Ca}$  channel plays important roles in the physiology of many cells (cf. Introduction), and agents that block  $IK_{Ca}$  channel activity have been proposed as potential therapeutic agents for sickle cell anaemia, cystic fibrosis, secretory diarrhoea, autoimmune diseases and restenosis (Jensen et al., 2001; Kohler et al., 2003). NPPB may well provide a template for designing more selective  $IK_{Ca}$  channel inhibitory compounds for clinical use.

#### References

- Bocchini, V., Casalone, R., Collini, P., Rebel, G., Lo Curto, F., 1991. Changes in glial fibrillary acidic protein and karyotype during culturing of two cell lines established from human glioblastoma multiforme. *Cell Tissue Res.* 265, 73–81.
- Castle, N.A., 1999. Recent advances in the biology of small conductance calcium-activated potassium channels. *Perspect. Drug Discov. Des.* 15, 131–154.
- Doughty, J.M., Miller, A.L., Langton, P.D., 1998. Non-specificity of chloride channel blockers in rat cerebral arteries: block of the L-type calcium channel. *J. Physiol.* 507, 433–439.

- Eskandari, S., Zampighi, G.A., Leung, D.W., Wright, E.M., Loo, D.D., 2002. Inhibition of gap junction hemichannels by chloride channel blockers. *J. Membr. Biol.* 185, 93–102.
- Fioretti, B., Catacuzzeno, L., Sciacaluga, M., Castigli, E., Franciolini, F., 2004.  $\text{Ca}^{2+}$ -activated K channels in glioblastoma GL-15 human cell line and their distinct modulation by ERK1/2. *Pflugers Arch.* (Abstr. in press).
- Gavrilova-Ruch, O., Schonherr, K., Gessner, G., Schonherr, R., Klapperstuck, T., Wohlrab, W., Heinemann, S.H., 2002. Effects of imipramine on ion channels and proliferation of IGR1 melanoma cells. *J. Membr. Biol.* 188, 137–149.
- Ghanshani, S., Wulff, H., Miller, M.J., Rohm, H., Neben, A., Gutman, G.A., Cahalan, M.D., Chandy, K.G., 2000. Up-regulation of the IKCa1 potassium channel during T-cell activation. Molecular mechanism and functional consequences. *J. Biol. Chem.* 275, 37137–37149.
- Gribkoff, V.K., Lum-Ragan, J.T., Boissard, C.G., Post-Munson, D.J., Meanwell, N.A., Starrett Jr., J.E., Kozlowski, E.S., Romine, J.L., Trojnacki, J.T., McKay, M.C., Zhong, J., Dworetzky, S.I., 1996. Effects of channel modulators on cloned large-conductance calcium-activated potassium channels. *Mol. Pharmacol.* 50, 206–217.
- Illek, B., Fischer, H., Kreusel, K.M., Hegel, U., Clauss, W., 1992. Volume-sensitive basolateral  $\text{K}^+$  channels in HT-29/B6 cells: block by lidocaine, quinidine, NPPB, and  $\text{Ba}^{2+}$ . *Am. J. Physiol.* 263, C674–C683.
- Jensen, B.S., Strobaek, D., Christophersen, P., Jorgensen, T.D., Hansen, C., Silahatoglu, A., Olesen, S.P., Ahring, P.K., 1998. Characterization of the cloned human intermediate-conductance  $\text{Ca}^{2+}$ -activated  $\text{K}^+$  channel. *Am. J. Physiol.* 275, C848–C856.
- Jensen, B.S., Strobaek, D., Olesen, S.P., Christophersen, P., 2001. The  $\text{Ca}^{2+}$ -activated  $\text{K}^+$  channel of intermediate conductance: a molecular target for novel treatments? *Curr. Drugs, Targets* 2, 401–422.
- Jentsch, T.J., Stein, V., Weinreich, F., Zdebik, A.A., 2002. Molecular structure and physiological function of chloride channels. *Physiol. Rev.* 82, 503–568.
- Khanna, R., Roy, L., Zhu, X., Schlichter, L.C., 2001.  $\text{K}^+$  channels and the microglial respiratory burst. *Am. J. Physiol., Cell Physiol.* 280, C796–C806.
- Kohler, R., Wulff, H., Eichler, I., Kneifel, M., Neumann, D., Knorr, A., Grgic, I., Kampfe, D., Si, H., Wibawa, J., Real, R., Borner, K., Brakemeier, S., Orzechowski, H.D., Reusch, H.P., Paul, M., Chandy, K.G., Hoyer, J., 2003. Blockade of the intermediate-conductance calcium-activated potassium channel as a new therapeutic strategy for restenosis. *Circulation* 108, 1119–1125.
- Li, J.H., Spence, K.T., Dargis, P.G., Christian, E.P., 2000. Properties of  $\text{Ca}^{2+}$ -release-activated  $\text{Ca}^{2+}$  channel block by 5-nitro-2-(3-phenylpropylamino)-benzoic acid in Jurkat cells. *Eur. J. Pharmacol.* 394, 171–179.
- Okada, Y., Maeno, E., Shimizu, T., Dezaki, K., Wang, J., Morishima, S., 2001. Receptor-mediated control of regulatory volume decrease (RVD) and apoptotic volume decrease (AVD). *J. Physiol.* 532, 3–16.
- Ransom, C.B., O'Neal, J.T., Sontheimer, H., 2001. Volume-activated chloride currents contribute to the resting conductance and invasive migration of human glioma cells. *J. Neurosci.* 21, 7674–7683.
- Richards, N.W., Dawson, D.C., 1993. Selective block of specific  $\text{K}^+$ -conducting channels by diphenylamine-2-carboxylate in turtle colon epithelial cells. *J. Physiol.* 462, 715–734.
- Schultz, B.D., Singh, A.K., Devor, D.C., Bridges, R.J., 1999. Pharmacology of CFTR chloride channel activity. *Physiol. Rev.* 79, S109–S144.
- Schwab, A., 2001. Ion channels and transporters on the move. *News Physiol. Sci.* 16, 29–33.
- Vergara, C., Latorre, R., Marrion, N.V., Adelman, J.P., 1998. Calcium-activated potassium channels. *Curr. Opin. Neurobiol.* 8, 321–329.
- Wang, J., Morishima, S., Okada, Y., 2003. IK channels are involved in the regulatory volume decrease in human epithelial cells. *Am. J. Physiol., Cell Physiol.* 284, C77–C84.
- Warth, R., Hamm, K., Bleich, M., Kunzelmann, K., Von Hahn, T., Schreiber, R., Ullrich, E., Mengel, M., Trautmann, N., Kindle, P., Schwab, A., Greger, R., 1999. Molecular and functional characterization of the small  $\text{Ca}^{2+}$ -regulated  $\text{K}^+$  channel (rSK4) of colonic crypts. *Pflugers Arch.* 438, 437–444.
- Wieland, S.J., Gong, Q.H., Chou, R.H., Brent, L.H., 1992. A lineage-specific  $\text{Ca}^{2+}$ -activated  $\text{K}^+$  conductance in HL-60 cells. *Biol. Chem.* 267, 15426–15431.